European Review for Medical and Pharmacological Sciences 2019; 23 (3 Suppl): 9-16

Role of miR-21 in rats with proliferative diabetic retinopathy *via* TGF-β signaling pathway

H.-D. LOU[1], S.-Y. WANG[2], T. GUO[3], Y. YANG[4]

[1]Department of Ophthalmology, Weifang Eye Hospital, Weifang, China
[2]Department of Ophthalmology, Shandong Gaomi People's Hospital, Gaomi, China
[3]Department of Ophthalmology, Weifang Maternal and Child Health Care Hospital, Weifang, China
[4]Department of Endocrinology, Weifang Second People's Hospital, Weifang, China

Abstract. – OBJECTIVE: To explore the effects of miR-21 on the rats with proliferative diabetic retinopathy by regulating the transforming growth factor-beta (TGF-β) signaling pathway.

MATERIALS AND METHODS: A total of 36 Sprague-Dawley rats were randomly divided into the normal group (n=12), model group (n=12), and inhibitor group (TGF-β signaling inhibitor) (n=12). No treatment was performed in the normal group, the diabetic retinopathy model was established in the model group, and the model was established in the inhibitor group after the intraperitoneal injection of the inhibitor. Then, the materials were sampled for detection. In each group, the retinal morphology was observed *via* hematoxylin-eosin (HE) staining, the expressions of TGF-β1 and Smad3 were detected *via* immunohistochemistry, the relative protein expression levels of phosphorylated Smad3 (p-Smad3) and TGF-β were determined *via* Western blotting, the expression of miR-21 was detected *via* quantitative Polymerase Chain Reaction (qPCR), and the hemodynamic indicators of the ocular tissues were detected using the color Doppler ultrasonography.

RESULTS: The HE staining results revealed that the rats in the model group had evident retinal damage, which could be effectively improved using the inhibitor. According to the immunohistochemistry detection results, the positive expression level of TGF-β1 was substantially raised in both model group and inhibitor group compared with that in the normal group ($p<0.05$), and it was notably lower in the inhibitor group than that in the model group ($p<0.05$). Moreover, the three groups did not differ in the positive expression level of Smad3 ($p>0.05$). The Western blotting results showed that the model and inhibitor groups had remarkably higher relative protein expression levels of p-Smad3 and TGF-β1 than the normal group ($p<0.05$), and they were markedly lowered in the inhibitor group compared with those in the model group ($p<0.05$). According to the qPCR results, the expression level of miR-21 was notably elevated in both model group and inhibitor group compared with that in the normal group ($p<0.05$), and there was no difference in the expression level of miR-21 between the former two groups ($p>0.05$). Finally, based on the color Doppler ultrasonography findings, the levels of the hemodynamic indicators substantially declined in both model group and inhibitor group compared with those in the normal group ($p<0.05$), and they were notably higher in the inhibitor group than those in the model group.

CONCLUSIONS: We found that miR-21 regulates the TGF-β signaling pathway to affect the hemodynamics in the rats with proliferative diabetic retinopathy.

Key Words:
Diabetic retinopathy, MiR-21, TGF-β signaling pathway.

Introduction

The morbidity rate of diabetic retinopathy, as an important complication of diabetes, has been increasingly higher. In particular, with the changes in people's lifestyle and living environments, as well as improvement in people's standard of living, the high morbidity rate of diabetes enables the incidence rate of diabetic retinopathy to gradually increase[1,2]. Diabetic retinopathy-induced retinal damage affects the visual acuity of patients, causing vision loss and blurred vision to patients in mild cases. On the other hand, in severe cases, it will make the patients lose labor capacity due to blindness, thereby imposing heavy economic burdens on the patients, their families, and the society[3,4]. As the studies on diabetic retinopathy continue to be deepened, it has been realized by researchers that the pathogenesis of this disease involves a series of complex pathological

Corresponding Author: Yan Yang, MM; e-mail: 94117782@qq.com

reactions, including vascular endothelial injury, decrease in pericytes, progressive thickening of vascular basement membranes, microaneurysm formation, and neovascularization, thereby severely impairing retinal endothelial function.

The transforming growth factor-beta (TGF-β), which is an important cytokine widely expressed and evenly distributed in the eyes, can be abnormally highly expressed upon stimulation by high blood glucose and other factors. Some reports[5,6] have suggested that TGF-β shows an aberrantly high expression in the serum of the diabetes patients, and its content is raised as the diabetic retinopathy is aggravated in the patients, indicating that TGF-β is closely associated with diabetic retinopathy. The TGF-β-mediated signaling pathway regulates fibrosis to play an important role in diabetic retinopathy.

As an important non-coding ribonucleic acid (RNA), microRNA (miR)-21 has crucial regulatory effects on several downstream signal transduction pathways in cells, thereby modulating the occurrence and development of multiple diseases[7]. Therefore, the present work aims to explore the influence of miR-21 on the rats with proliferative diabetic retinopathy by regulating the TGF-β pathway.

Material and Methods

Experimental Animals

A total of 36 SPF laboratory Sprague-Dawley (SD) rats aged 1 month old (Shanghai SLAC Laboratory Animal Co., Ltd., certificate No.: SCXK Hu 2014-0003, Shanghai, China) were fed with normal diet and sterile filtered water daily in the Experimental Animal Center under 12/12 h of light-dark cycle at normal room temperature and humidity. This study was approved by the Animal Ethics Committee of Weifang Eye Hospital Animal Center.

Experimental Reagents and Instruments

The main reagents and instruments used were: streptozotocin (Sigma Aldrich, St. Louis, MO, USA), TGF-β signaling inhibitor HY-P0118 (MCE, Billerica, MA, USA), primary antibodies: anti-phosphorylated Smad3 (p-Smad3) antibody, anti-Smad3 antibody, anti-TGF-β1 antibody and secondary antibodies (Abcam, Cambridge, MA, USA), hematoxylin-eosin (HE) staining kit, AceQ quantitative Polymerase Chain Reaction (qPCR) SYBR Green Master Mix kit and HiScript II Q reverse transcription (RT) SuperMix for qPCR [+genomic deoxyribonucleic acid (+gDNA) wiper] kit (Vazyme Biotechnology, Nanjing, China), optical microscope (Leica DMI 4000B/DFC425C, Germany; Thermo Fisher Scientific, Waltham, MA, USA) and fluorescence quantitative PCR instrument (ABI 7500, Thermo Fisher Scientific, Waltham, MA, USA).

Animal Grouping

Thirty-six SD rats were randomly divided into normal group (n=12), model group (n=12) and inhibitor group (TGF-β signaling inhibitor) (n=12) using a random number table. They were adaptively fed in the Experimental Animal Center for 7 d and then, used in subsequent experiments.

The rats in the normal group were normally fed without any treatments, those in the model group were used for the establishment of the diabetic retinopathy model and sacrificed after successful modeling, and those in the inhibitor group were firstly intraperitoneally injected with HY-P0118 (TGF-β signaling inhibitor) at the dose of 70 μg/300 g and then used for modeling.

Establishment of Diabetic Retinopathy Model

The rats were firstly intraperitoneally injected with 1% streptozotocin solution prepared at a dose of 60 mg/kg, and 3 d later, the blood was drawn from the caudal veins of the rats to detect blood glucose, with blood glucose >16.7 mmol/L as the criterion for successful modeling.

Sampling

After all the rats were successfully anesthetized, the samples were directly taken from 6 rats in each group, namely the retinal tissues which were directly obtained, rinsed with normal saline, placed in EP tubes and stored at -80°C for subsequent Western blotting and qPCR. The remaining 6 rats in each group were fixed through perfusion for sampling as follows: the thoracic cavity of the rats was sheared open to expose the heart, and the left atrial appendage was perfused with 400 mL of 4% paraformaldehyde. Then, the retinal tissues were taken out, soaked, and fixed in 4% paraformaldehyde for immunohistochemistry detection and hematoxylin-eosin staining (HE; Boster, Wuhan, China).

HE Staining

The tissues embedded in paraffin in advance were made into 5 μm-thick sections, extended, mounted, and baked in warm water at 42°C, and

prepared into paraffin-embedded tissue sections. Then, these sections were immersed in xylene solution and gradient ethanol for routine deparaffinization and dehydration, successively. Subsequently, the resulting sections were stained with hematoxylin solution at room temperature for 10 min, rinsed, and soaked in the hydrochloric acid solution for several seconds for differentiation. After rinsing, they were reacted with eosin staining solution for 30 s, and re-hydrated in gradient ethanol. Finally, the sections were observed for proper color development and sealed.

Immunohistochemistry

The pre-paraffin-embedded tissues were sliced to 5 μm-thick sections, placed in warm water at 42°C for extending, mounting, baking, and prepared into paraffin-embedded tissue sections. Then, the tissue sections were routinely deparaffinized and dehydrated through soaking in xylene solution and gradient ethanol, successively. Subsequently, they were immersed in citrate buffer and heated repeatedly using a microwave oven for 3 times (heating for 3 min and braising for 5 min per time) for complete antigen retrieval. After rinsing, the tissue sections were added dropwise with endogenous peroxidase blocker, reacted for 10 min, rinsed, and sealed in goat serum for 20 min. With the goat serum sealing solution discarded, the resulting sections were incubated with the anti-TGF-β1 and Smad3 primary antibodies (1:200) in a refrigerator at 4°C overnight. On the next day, the sections rinsed were added dropwise with the secondary antibody solution, reacted for 10 min and fully rinsed, followed by reaction with a streptavidin-peroxidase solution for 10 min and color development using diaminobenzidine (DAB; Solarbio, Beijing, China). Finally, the sections were counter-stained using hematoxylin, sealed, and observed.

Western Blotting

The cryopreserved retinal tissues were added with lysis buffer, bathed on ice for 1 h and then centrifuged at 14,000 g in a centrifuge for 10 min, followed by protein quantification using bicinchoninic acid (BCA; Pierce, Rockford, IL, USA). The absorbance of proteins was measured using a microplate reader, and the standard curve was plotted to calculate the concentration of the proteins in the tissues. Then, the proteins were denaturalized and isolated *via* dodecyl sulfate, sodium salt-polyacrylamide gel electrophoresis (SDS-PAGE), which stopped when the marker proteins were observed to stay at the bottom of the glass plate in a straight line. Following electrophoresis, the resulting proteins were transferred onto a polyvinylidene difluoride (PVDF) membrane (Roche, Basel, Switzerland) and reacted with the sealing solution for 1.5 h, followed by successive incubation with the anti-p-Smad3 primary antibody (1:1,000), anti-TGF-β1 primary antibody (1:1,000) and secondary antibodies (1:1,000). After rinsing, the color was fully developed by reacting with the chemiluminescent reagent for 1 min in the dark.

Quantitative Real Time-Polymerase Chain Reaction (qRT-PCR)

The total RNAs were firstly extracted from tissue specimens and reversely transcribed into complementary DNAs (cDNAs) using the RT kit (TaKaRa, Otsu, Shiga, Japan). Subsequently, the qPCR was performed in the system (20 μL) under the following conditions: reaction at 51°C for 2 min, pre-degeneration at 96°C for 10 min, degeneration at 96°C for 10 s and annealing at 60°C for 30 s reaction, for 40 cycles in total. The relative expression levels of the related messenger RNAs (mRNAs) were calculated with glyceraldehyde-3-phosphate dehydrogenase (GAPDH) as the internal reference. The primer sequences are listed in Table I.

Detection of Retinal Hemodynamic Indicators

The color Doppler ultrasonography was performed to detect the hemodynamic indicators in the right eye of each rat, including the peak

Table I. Primer sequence.

Gene	Primer sequence
MiR-21	Forward: 5' TCCACCAAGAAGCTGAGCGAG 3' Reverse: 5' GTCCAGCCCATGATGGTTCT 3'
GAPDH	Forward: 5' ACGGCAAGTTCAACGGCACAG 3' Reverse: 5' GAAGACGCCAGTAGACTCCACGAC 3'

systolic velocity, end-diastolic velocity, and average velocity and the blood velocity in the central retinal vein.

Statistical Analysis

In this work, the Statistical Product and Service Solutions (SPSS) 20.0 (IBM Corp., Armonk, NY, USA) software was used for statistical analysis. The enumeration data were expressed as mean ± standard deviation. The *t*-test, corrected *t*-test, and nonparametric test were performed for data conforming to normal distribution and homogeneity of variance, those meeting normal distribution and heterogeneity of variance and those not in line with normal distribution and homogeneity of variance, respectively. Moreover, the rank-sum test and the Chi-square test were conducted for ranked data and count data, respectively. $p<0.05$ indicated statistical significance.

Results

Retinal Morphology Observed Via HE Staining

As shown in Figure 1, the normal group exhibited regularly arranged retinal cells with normal morphology, round orderly-arranged ganglion cells, and normally stained and clear cell nuclei without evident damages, while the model group had disorderedly arranged the retinal cells with changed morphology, some of which were loosely arranged, and poorly stained the cell nuclei with nuclear fragmentation and even disappearance, as well as more visible cavitations in some of them. Besides, the inhibitor group had more orderly-arranged retinal cells with improved morphology compared with the model group.

Immunohistochemistry Detection Results

The cells showing positive expression are chocolate brown in Figure 2. The normal group had fewer cells, exhibiting positive expression than the model group. According to the statistical results (Figure 3), compared with that in the normal group, the average optical density of the positively expressed TGF-β was substantially raised in the model group and inhibitor group, showing statistically significant differences ($p<0.05$), and it was higher in the inhibitor group than that in the model group, with a statistically significant difference ($p<0.05$). Additionally, there were no significant differences in the average optical density of positively expressed Smad3 among the three groups ($p>0.05$).

Western Blotting Detection Results

As shown in Figure 4, the normal group had lower protein expression levels of p-Smad3 and TGF-β1 than the model group. According to the statistical results (Figure 5), the relative protein expression levels of p-Smad3 and TGF-β1 substantially rose in the model and inhibitor groups, compared with those in the normal group, and the differences were statistically significant ($p<0.05$). In addition, they were notably lower in the inhibitor group than those in the model group, showing statistically significant differences ($p<0.05$).

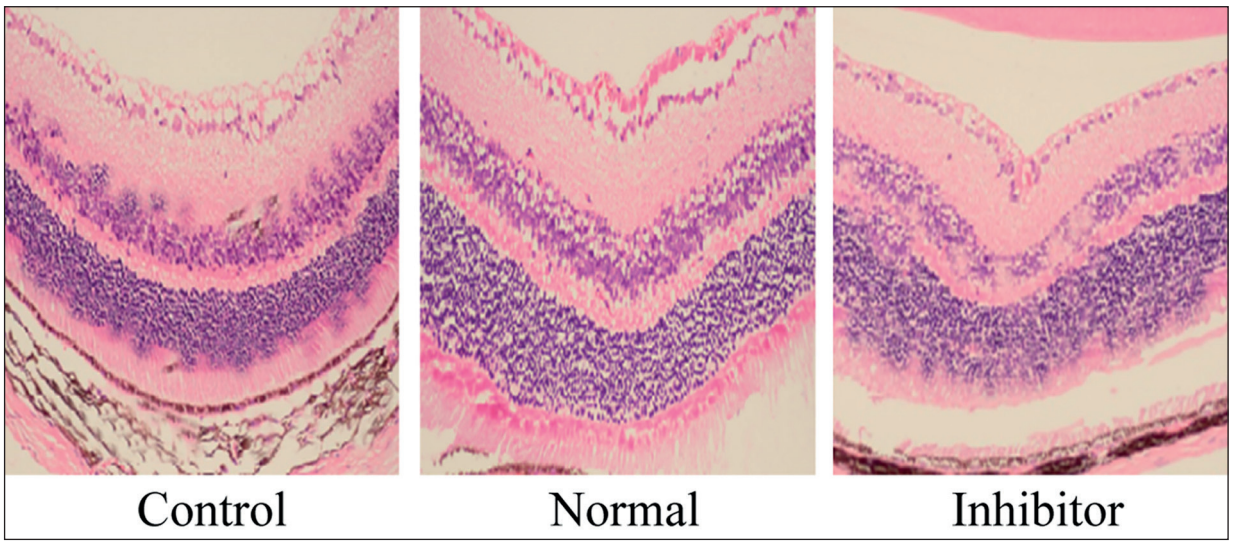

Figure 1. Retinal morphology observed *via* HE staining (×200).

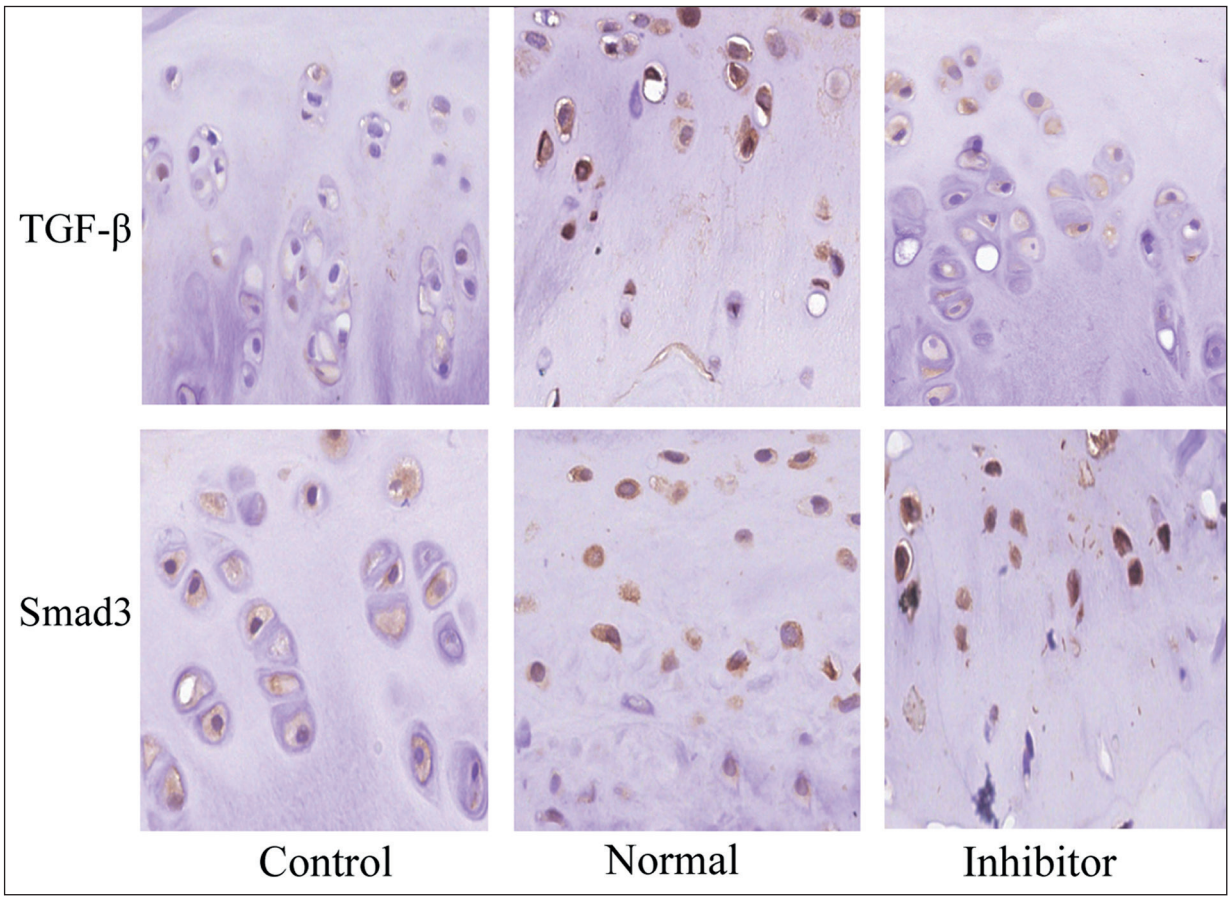

Figure 2. Immunohistochemistry detection results (×200).

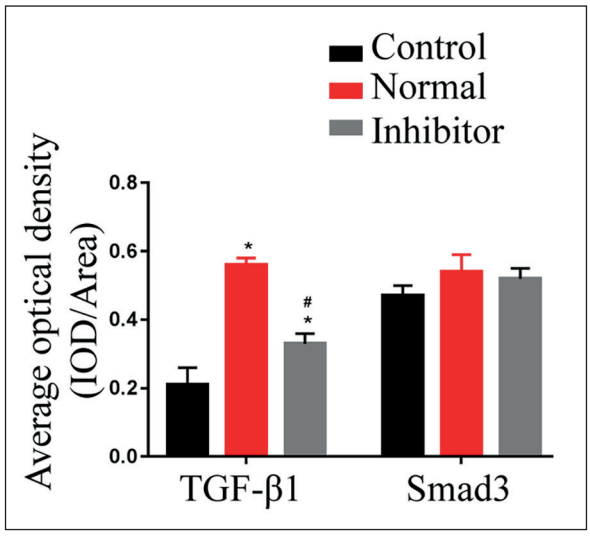

Figure 3. Average optical density of tissues showing positive expression in each group.

QPCR Results

Compared with the normal group, the model group had a remarkably raised expression level of miR-21, with a statistically significant difference ($p<0.05$), and the comparison indicated no significant difference in the expression level of miR-21 between the model group and the inhibitor group ($p>0.05$) (Figure 6).

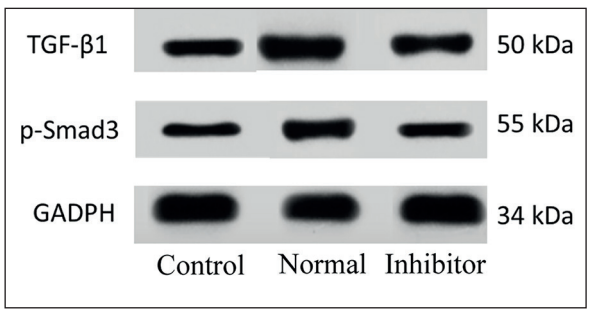

Figure 4. Expressions of related proteins detected *via* Western blotting.

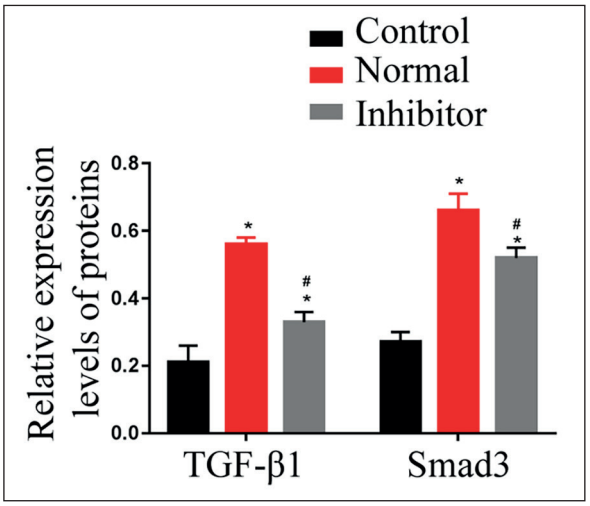

Figure 5. Relative expression levels of proteins in each group.

Hemodynamic Indicators Detected

According to the detection results (Figure 7), both the model group and inhibitor group exhibited notably decreased peak systolic velocity, end-diastolic velocity, and average velocity in the central retinal artery and blood velocity in the central retinal vein compared with the normal group, displaying statistically significant differences (p<0.05), and they were substantially higher in the inhibitor group than those in the model group with statistically significant differences (p<0.05).

Discussion

As an important complication of diabetes, diabetic retinopathy can cause severe and even irreversible damage to the vision of patients, making it one of the leading causes of blindness in patients. In particular, as the society develops and humans' living standard improves, diabetic retinopathy has become more and more common with the increase in the morbidity rate of diabetes, so that most diabetes patients ultimately lose labor capacity due to blindness[8,9]. TGF-β and TGF-β-mediated signaling pathways play an important role in the pathogenesis of diabetic retinopathy. Moreover, TGF-β can be synthesized and secreted by multiple intraocular histiocytes, including hepatocytes, lens epithelial cells, iris cells, and ciliary epithelial cells[10,11]. Further investigations[12,13] have suggested that TGF-β and TGF-β-mediated signaling pathways can exert important regulatory effects on the growth and differentiation of the cells, for example, as crucial inducing factors for tissue fibrosis, they can promote the proliferation of fibroblasts, ultimately causing tissue fibrosis. Additionally, both TGF-β and Smad3 are crucial molecules in the TGF-β signaling pathway. TGF-β1, once stimulated by the high blood glucose in the ocular tissues, can be abnormally highly expressed, thereby transmitting the cell signals to exert its biological effects, especially the intense stimulating effect on the downstream Smad3 that can be activated and further phosphorylated, and has no evident biological activity under non-phosphorylation state[14,15]. P-Smad3 will be formed after phosphorylating Smad3, and then enters the nucleus to transmit cell signals and enable numerous transcription factors to transcribe, further inducing retinal fibrosis, and affecting vision *via* the

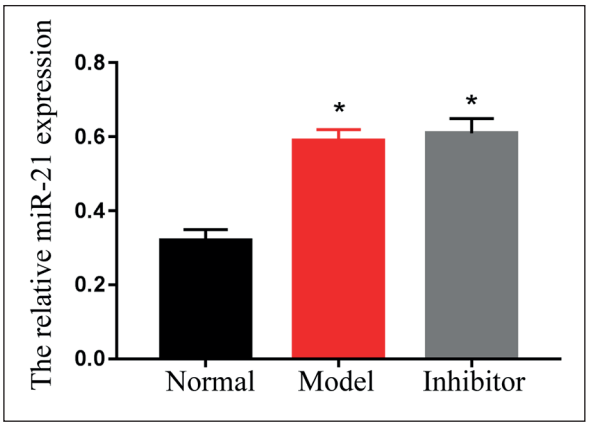

Figure 6. Relative expression level of miR-21 determined *via* qPCR.

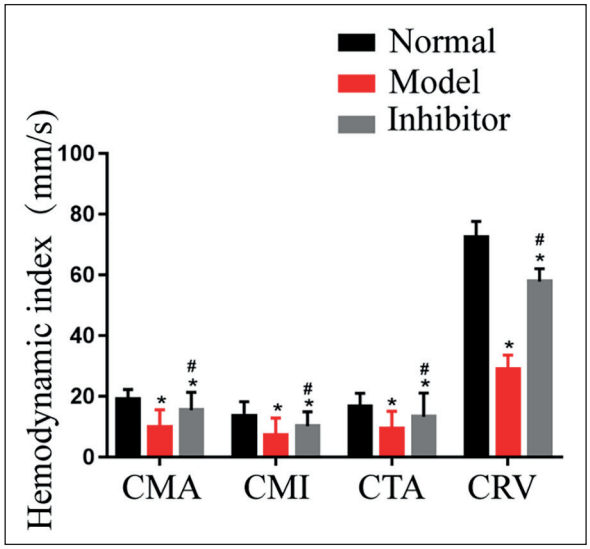

Figure 7. Hemodynamic indicators in each group.

influence on the blood circulation system[16,17]. According to the results of the present investigation, TGF-β1 and p-Smad3 were aberrantly highly expressed in the retinal tissues of the diabetic retinopathy model rats and higher than those in the normal rats, suggesting that the TGF-β signaling pathway is activated in the retinal tissues of the diabetic retinopathy model rats to induce fibrosis in such tissues, which may be one of the causes of the decreases in the ocular hemodynamic indicators in the model rats.

MiR-21, a non-coding RNA, is currently considered to play a critical regulatory role in organisms, and has been confirmed to bear close relationships with the onset of multiple diseases as well. Some works[18,19] have demonstrated that miR-21 pairs with the untranslated regions of the downstream genes to degrade or suppress the downstream mRNAs, thereby modulating transcription and such pathological processes as cell proliferation, differentiation, and apoptosis. According to the findings of another study, miR-21 is closely associated with the occurrence and development of multiple diseases, and is recognized as an important regulator therein. In addition, it is capable of regulating numerous cellular signaling pathways to exert important effects and influences on numerous pathological reactions in diseases[20]. In this report, it was found that the expression level of miR-21 was substantially higher in the retinal tissues in the diabetic retinopathy model rats than that in normal rats, implying that miR-21 is abnormally expressed in the retinal tissues of the diabetic retinopathy model rats and involved in the onset of diabetic retinopathy. Meanwhile, the results of the present analysis revealed that the TGF-β signaling pathway inhibitor remarkably weakened the role of miR-21 in diabetic retinopathy and improved the ocular hemodynamics in the diabetic retinopathy model rats, illustrating that miR-21 regulates the TGF-β signaling pathway to participate in the onset of the diabetic retinopathy. Therefore, it is concluded that miR-21 affects the hemodynamics in the rats with proliferative diabetic retinopathy by regulating the TGF-β signaling pathway.

Conclusions

We showed that miR-21 affects the hemodynamics in the rats with proliferative diabetic retinopathy by regulating the TGF-β signaling pathway.

Conflict of Interest

The Authors declare that they have no conflict of interests.

References

1) Ding J, Wong TY. Current epidemiology of diabetic retinopathy and diabetic macular edema. Curr Diab Rep 2012; 12: 346-354.
2) Cohen SR, Gardner TW. Diabetic retinopathy and diabetic macular edema. Dev Ophthalmol 2016; 55: 137-146.
3) Ting DS, Cheung GC, Wong TY. Diabetic retinopathy: global prevalence, major risk factors, screening practices and public health challenges: a review. Clin Exp Ophthalmol 2016; 44: 260-277.
4) Stitt AW, Curtis TM, Chen M, Medina RJ, McKay GJ, Jenkins A, Gardiner TA, Lyons TJ, Hammes HP, Simo R, Lois N. The progress in understanding and treatment of diabetic retinopathy. Prog Retin Eye Res 2016; 51: 156-186.
5) Yue Y, Meng K, Pu Y, Zhang X. Transforming growth factor beta (TGF-β) mediates cardiac fibrosis and induces diabetic cardiomyopathy. Diabetes Res Clin Pract 2017; 133: 124-130.
6) Dagher Z, Gerhardinger C, Vaz J, Goodridge M, Tecilazich F, Lorenzi M. The Increased Transforming Growth Factor-β Signaling Induced by Diabetes Protects Retinal Vessels. Am J Pathol 2017; 187: 627-638.
7) Blum W, Garzon R, Klisovic RB, Schwind S, Walker A, Geyer S, Liu S, Havelange V, Becker H, Schaaf L, Mickle J, Devine H, Kefauver C, Devine SM, Chan KK, Heerema NA, Bloomfield CD, Grever MR, Byrd JC, Villalona-Calero M, Croce CM, Marcucci G. Clinical response and miR-29b predictive significance in older AML patients treated with a 10-day schedule of decitabine. Proc Natl Acad Sci U S A 2010; 107: 7473-7478.
8) Gulshan V, Peng L, Coram M, Stumpe MC, Wu D, Narayanaswamy A, Venugopalan S, Widner K, Madams T, Cuadros J, Kim R, Raman R, Nelson PC, Mega JL, Webster DR. Development and validation of a deep learning algorithm for detection of diabetic retinopathy in retinal fundus photographs. JAMA 2016; 316: 2402-2410.
9) Freiberg FJ, Pfau M, Wons J, Wirth MA, Becker MD, Michels S. Optical coherence tomography angiography of the foveal avascular zone in diabetic retinopathy. Graefes Arch Clin Exp Ophthalmol 2016; 254: 1051-1058.
10) Qiao YC, Chen YL, Pan YH, Ling W, Tian F, Zhang XX, Zhao HL. Changes of transforming growth factor beta 1 in patients with type 2 diabetes and diabetic nephropathy: A PRISMA-compliant systematic review and meta-analysis. Medicine (Baltimore) 2017; 96: e6583.
11) Kim DJ, Kang JM, Park SH, Kwon HK, Song SJ, Moon H, Kim SM, Seo JW, Lee YH, Kim YG, Moon JY, Lee

SY, Son Y, Lee SH. Diabetes aggravates post-ischaemic renal fibrosis through persistent activation of TGF-beta1 and Shh signalling. Sci Rep 2017; 7: 16782.

12) Kilari S, Yang B, Sharma A, McCall DL, Misra S. Increased transforming growth factor beta (TGF-beta) and pSMAD3 signaling in a murine model for contrast induced kidney injury. Sci Rep 2018; 8: 6630.

13) van der Velden JL, Wagner DE, Lahue KG, Abdalla ST, Lam YW, Weiss DJ, Janssen-Heininger YMW. TGF-β1-induced deposition of provisional extracellular matrix by tracheal basal cells promotes epithelial-to-mesenchymal transition in a c-Jun NH2-terminal kinase-1-dependent manner. Am J Physiol Lung Cell Mol Physiol 2018; 314: L984-L997.

14) Xia W, Lo CM, Poon R, Cheung TT, Chan A, Chen L, Yang S, Tsao G, Wang XQ. Smad inhibitor induces CSC differentiation for effective chemosensitization in cyclin D1- and TGF-β/Smad-regulated liver cancer stem cell-like cells. Oncotarget 2017; 8: 38811-38824.

15) Xu L, Cui WH, Zhou WC, Li DL, Li LC, Zhao P, Mo XT, Zhang Z, Gao J. Activation of Wnt/β-catenin signalling is required for TGF-β/Smad2/3 signalling during myofibroblast proliferation. J Cell Mol Med 2017; 21: 1545-1554.

16) Xie Y, Hu JZ, Shi ZY. MiR-181d promotes steroid-induced osteonecrosis of the femoral head by targeting SMAD3 to inhibit osteogenic differentiation of hBMSCs. Eur Rev Med Pharmacol Sci 2018; 22: 4053-4062.

17) Khalil H, Kanisicak O, Prasad V, Correll RN, Fu X, Schips T, Vagnozzi RJ, Liu R, Huynh T, Lee SJ, Karch J, Molkentin JD. Fibroblast-specific TGF-β-Smad2/3 signaling underlies cardiac fibrosis. J Clin Invest 2017; 127: 3770-3783.

18) Zeng Y, Yi R, Cullen BR. Recognition and cleavage of primary microRNA precursors by the nuclear processing enzyme Drosha. EMBO J 2005; 24: 138-148.

19) Lee Y, Ahn C, Han J, Choi H, Kim J, Yim J, Lee J, Provost P, Radmark O, Kim S, Kim VN. The nuclear RNase III Drosha initiates microRNA processing. Nature 2003; 425: 415-419.

20) Zheng P, Chen L, Yuan X, Luo Q, Liu Y, Xie G, Ma Y, Shen L. Exosomal transfer of tumor-associated macrophage-derived miR-21 confers cisplatin resistance in gastric cancer cells. J Exp Clin Cancer Res 2017; 36: 53.